Journal of Physics:
Conference Series

PAPER • OPEN ACCESS

Traversable Schwarzschild-like Wormholes in Isotropic Coordinate

To cite this article: Arista Romadani *et al* 2026 *J. Phys.: Conf. Ser.* **3238** 012048

Journal of Physics: Conference Series **3238** (2026) 012048 doi:10.1088/1742-6596/3238/1/012048

Traversable Schwarzschild-like Wormholes in Isotropic Coordinate

Arista Romadani[1,2,*], **Bintoro Anang Subagyo**[1], **Agus Purwanto**[1], **Apriadi Salim Adam**[3]

[1]Department of Physics, Sepuluh Nopember Institute of Technology, Kampus ITS Sukolilo, Surabaya, 60111, Indonesia
[2]Department of Physics, Universitas Islam Negeri Maulana Malik Ibrahim Malang, Malang 65144, Indonesia
[3]Research Center for Quantum Physics, National Research and Innovation Agency (BRIN), South Tangerang 15314, Indonesia

*Corresponding author: arista.romadani@uin-malang.ac.id

Abstract. The characteristics of a Schwarzschild-like wormhole are always challenging, with the main issues being stability and traversability. In this study, we construct a metric for a traversable Schwarzschild-like wormhole in isotropic coordinates and analyze the behavior of the traversable wormhole. We demonstrate the embedding diagram of a Schwarzschild-like wormhole to visualize the throat of the wormhole, showing two distinct spacetime properties. We also identify the geodesic of a particle in a Schwarzschild-like wormhole spacetime. The trajectory of particles moving to the throat of Schwarzschild-like spacetime is determined by angular momentum and kinetic energy. The angular momentum shows how particles move into the throat, while the kinetic energy determines whether the particle can reach the throat or not. This work could provide a promising approach to investigating the dynamics of particles and the stability conditions near Schwarzschild-like wormholes, thereby producing a deeper understanding of traversability and providing observational evidence.

Keywords: Schwarzschild-like, wormhole, isotropic, traversable, geodesic.

1. Introduction

Einstein's field theory allows for a straightforward and intriguing solution, namely the proposal of a tunnel connecting two asymptotically flat universes or two sections of an asymptotically flat universe within the same universe. Many scientists have become interested in it, with some seeking to explain its geometric properties and physical effects [1]. The tunnel in question is referred to as a wormhole. It was initially suggested by Flamm in 1916, who described it as a tunnel linking two spacetime regions based on the Schwarzschild solution analysis [2]. Weyl's 1928 work added to the understanding of wormhole spacetime's geometric structure, ultimately laying the groundwork for general relativity theory [3] [4]. Flamm and Weyl established the groundwork for connected spacetime geometry, the precursor to the Einstein-Rosen Bridge concept.

Einstein and Rosen (1935) introduced the concept of a spacetime tunnel—now known as the Einstein–Rosen bridge—as an exact solution to the Einstein field equations, connecting two identical regions of spacetime. This construction is widely regarded as the first theoretical example of a wormhole [5]. Besides serving as potential shortcuts connecting distant regions of spacetime, wormholes have also been considered as candidates for constructing time machines. For such applications, one requires a stable and traversable wormhole—one that can be crossed safely by observers—of the type proposed in [6]. The term wormhole itself was first introduced by Wheeler in 1957, who envisioned a tunnel-like structure in spacetime [7]. However, the discussed configurations were not physically traversable. Later, in 1963, Kerr discovered a solution describing a rotating black hole whose maximally extended spacetime contains a wormhole-like structure. This geometry is also non-traversable in practice, as the presence of horizons prevents safe passage [8, 9, 10]. All known wormhole geometries obtained as classical solutions of general relativity are non-traversable, as they inevitably develop horizons or pinch off too rapidly to permit passage.

The first explicit construction of a traversable wormhole was given by Morris and Thorne in 1988. In their seminal analysis, they formulated the geometric criteria that a wormhole must satisfy to allow safe passage by observers and obtained solutions for static, spherically symmetric, non-rotating spacetimes. By inserting this metric ansatz into Einstein's field equations, they demonstrated that maintaining such a wormhole necessarily requires matter sources that violate standard energy conditions [13]. By definition, a traversable wormhole allows two-way passage by observers or physical objects such as humans [14]. Although the Schwarzschild solution contains a wormhole structure in its maximally extended form, this geometry is non-traversable because an event horizon shields the throat and pinches off too rapidly for traversal. Avoiding horizons imposes restrictions on the redshift function of the metric. A convenient way to satisfy these conditions is to adopt a linear redshift function, which ensures regularity and prevents the formation of horizons [1]. This construction yields what is known as a Schwarzschild-style wormhole: a static geometry that retains the formal structure of the Schwarzschild metric while remaining horizonless and, therefore, traversable [15].

In Schwarzschild spacetime, the use of isotropic coordinates makes the presence of two spatial sheets, connected at the Schwarzschild throat—the Einstein–Rosen bridge —explicit. For Schwarzschild-like wormholes, these coordinates reveal a bridge configuration that similarly links two asymptotically flat regions. The isotropic representation highlights the geometric symmetry between the two sides of the wormhole. It remains a regular feature across the world horizon, making it a simple yet effective coordinate system for analyzing traversable geometries. In this work, we employ isotropic coordinates to describe the traversable wormhole and investigate both its linear stability and the geodesic trajectories of test particles traversing the throat.

In Schwarzschild spacetime, isotropic coordinates reveal the presence of two spatial sheets, connected at the Schwarzschild throat—the Einstein–Rosen bridge—explicitly. Similarly, for Schwarzschild-like wormholes, they reveal a bridge linking two asymptotically flat regions. This coordinate representation highlights the geometric symmetry of both sides of the wormhole and remains regular across the would-be horizon, making it a practical framework for analyzing traversable geometries. In this work, we construct a Schwarzschild-like traversable wormhole in isotropic coordinates, starting from a Schwarzschild-inspired metric under the assumption of spherical symmetry. We examine the geometric properties of the resulting configuration, including the structure of the throat, the absence of singularities, and the corresponding geodesics, and visualize its spatial geometry through an embedding diagram for both timelike and null trajectories. Finally, we analyze particle motion in this spacetime, showing how angular momentum and kinetic energy determine whether a particle reaches the throat and successfully traverses the wormhole.

Journal of Physics: Conference Series **3238** (2026) 012048 doi:10.1088/1742-6596/3238/1/012048

2. Schwarzschild-like Wormholes

Morris and Thorne metric is static, spherically symmetric, and asymptotically flat as follows:

$$ds^2 = e^{2\Phi(r)}dt^2 - \frac{dr^2}{1-\frac{b(r)}{r}} - r^2 d\Omega^2, \tag{1}$$

where the redshift function $\Phi(r)$ is associated with the gravitational effect in a wormhole spacetime and the shape function $b(r)$ is associated with the wormhole geometry. We assume that there is no tidal force, $\Phi(r) = 0$. If the redshift function requires $e^{2\Phi(r)} = 1 - \frac{r_0}{r}$, the metric will be a Schwarzschild wormhole. The function of $b(r)$ must satisfy $b(r) < r$ so that the wormhole is always open and traversable. If $b(r)$ is constant, the wormhole will not be traversable because it has a singularity at the throat. Next, we choose the linear shape function as follows: [1]

$$b(r) = \alpha + \beta r,$$

where α and β are free parameters.

By applying the condition of Schwarzschild $b(r_0) = r_0$, we get $\alpha = (1-\beta)r_0$ and the shape function becomes

$$b(r) = (1-\beta)r_0 + \beta r.$$

From this condition, we also obtain that the wormhole shape function has a minimum at $r = r_0$, where the wormhole throat is located. The throat is determined by the definition $b(r_{\text{th}}) = r_{\text{th}}$ producing a throat radius, $r_{\text{th}} = r_0$. The Morris-Thorne metric is written as

$$ds^2 = dt^2 - \frac{dr^2}{(1-\beta)\left(1-\frac{r_0}{r}\right)} - r^2 d\Omega^2, \tag{2}$$

where the radial coordinate covers the range $r_0 < r < \infty$, the angles satisfy $0 \leq \theta \leq \pi$ and $0 \leq \phi \leq 2\pi$, respectively. The metric in Eq. (2) is known as the Schwarzschild-like wormhole. Flare-out condition about the traversability of the wormhole implies that $0 < \beta < 1$.

The Kretschmann scalar curvatures K of the Schwarzschild-like wormhole are given by

$$K = \frac{2}{r^6}\left[2\beta^2 r^2 - 4\beta(\beta-1)rr_0 + 3(\beta-1)^2 r_0^2\right]. \tag{3}$$

Moreover, the Kretschmann scalar is divergent at $r = 0$, where this point is called a curvature singularity. However, the particle never reaches $r = 0$ because the radial range is allowed for $r > r_0$. The Kretschmann scalar is finite for $r > 0$, so that $r = r_0$ is a coordinate singularity. For $r \to \pm\infty$, the Kretschmann scalar vanishes and indicates that the wormhole is asymptotically flat at infinity.

Assuming that the source of matter passing through the wormhole is modelled by an anisotropic fluid where the energy-momentum tensor is defined as $T^{\nu}_{\mu} = diag(\rho, -p_r, -p_l, -p_l)$. We obtain the Einstein field equations as follows:

$$\begin{aligned} \kappa\rho(r) &= \frac{\beta}{r^2} \\ \kappa p_r(r) &= -\frac{(1-\beta)r_0 + \beta r}{r^3} \\ \kappa p_l(r) &= \frac{(1-\beta)r_0}{2r^3}, \end{aligned} \tag{4}$$

Journal of Physics: Conference Series **3238** (2026) 012048 doi:10.1088/1742-6596/3238/1/012048

where ρ is the energy density, p_r and p_l are the radial and lateral pressures, respectively. From the energy-momentum tensor component, we obtain that $\kappa(\rho+p_r)<0$ and the relation violates the null energy condition (NEC). The weak energy condition (WEC) requires $\rho\geq 0$ and $\rho+p_i\geq 0$, and they are not fulfilled because $\rho+p_r<0$. We compute that $\rho+p_r+2p_t<0$, so the strong energy condition (SEC) is also violated. The Dominant Energy Condition (DEC) requires $\rho\geq 0$ and $|p_i|\leq\rho$, and we have $\rho+p_r<0$, so the DEC is not satisfied in general (the violation for the typical $\beta<1$). We conclude that all energy conditions are violated in the Schwarzschild-like wormhole metric, and this violation allows the presence of exotic matter that produces energy with a negative value.

2.1. The Embedding of Schwarzschild-like Wormhole

In this section, we begin embedding a diagram of Schwarzschild-like wormhole spacetime by bringing it into the cylindrical coordinates (t, r_s, z, ϕ) with constant t and $\theta=\pi/2$, we have

$$dr_s^2+dz^2+r_s^2d\phi^2=\frac{dr^2}{(1-\beta)\left(1-\frac{r_0}{r}\right)}+r^2d\phi^2. \tag{5}$$

By comparing the two sides of Equation (5), we obtain the relation: $r_s=r$ and

$$\frac{dz^2}{dr_s^2}+1=\frac{1}{(1-\beta)\left(1-\frac{r_0}{r}\right)}\frac{dr^2}{dr_s^2}. \tag{6}$$

The above relations are written as follows:

$$\frac{dz}{dr}=\pm\sqrt{\frac{1}{(1-\beta)\Big(1-\dfrac{r_0}{r}\Big)}-1}=\pm\sqrt{\frac{\beta+(1-\beta)\dfrac{r_0}{r}}{(1-\beta)\Big(1-\dfrac{r_0}{r}\Big)}}. \tag{7}$$

Suppose that $u=\frac{r}{r_0}$ or $dr=r_0\,du$ with $u\geq 1$, we obtain

$$dz=\pm\frac{r_0}{\sqrt{1-\beta}}\sqrt{\frac{\beta u+(1-\beta)}{u-1}}\,du \tag{8}$$

and the solution of the differential equation can be solved by introducing $x=\sqrt{u-1}$ or $u=1+x^2$ and $du=2x\,dx$, so we have

$$\frac{dz}{dx}=\pm\frac{2r_0}{\sqrt{1-\beta}}\sqrt{1+\beta x^2}. \tag{9}$$

Using some techniques of integration in the following,

$$\int\sqrt{1+\beta x^2}\,dx=\frac{x}{2}\sqrt{1+\beta x^2}+\frac{1}{2\sqrt{\beta}}\ln\Big(\sqrt{\beta}\,x+\sqrt{1+\beta x^2}\Big) \tag{10}$$

the solution of Eq. (8) is written as

$$z(r)=\pm\frac{1}{\sqrt{1-\beta}}\left[\sqrt{r_0\,(r-r_0)+\beta\,(r-r_0)^2}+\frac{r_0}{\sqrt{\beta}}\ln\left(\sqrt{\frac{\beta}{r_0}\,(r-r_0)}+\sqrt{1+\frac{\beta}{r_0}\,(r-r_0)}\right)\right]. \tag{11}$$

Moreover, it is valid for $0<\beta<1$. For $\beta\to 0$, the Eq. (11) becomes $z(r)=\pm 2\sqrt{r_0(r-r_0)}$ and for $\beta<0$, the logarithmic term transforms into an inverse sine function because the argument of the logarithm becomes complex. Lastly, we show the embedding diagram of the Schwarzschild-like wormhole of Eq. (11) in Figure 1.

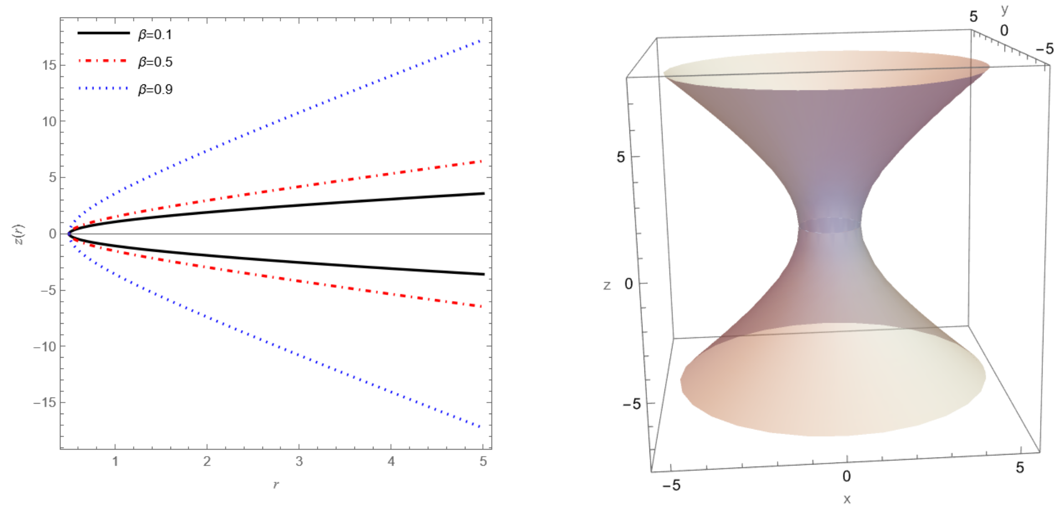

Figure 1. Embedding diagram of a Schwarzschild-like wormhole (a) 2D and (b) 3D

2.2. Geodesics of Schwarzschild-like Wormhole

The component of Schwarzschild-like metric from Eq. (2) is written as

$$g_{\alpha\beta} = \begin{pmatrix} 1 & 0 & 0 & 0 \\ 0 & -\frac{1}{(1-\beta)\left(1-\frac{r_0}{r}\right)} & 0 & 0 \\ 0 & 0 & -r^2 & 0 \\ 0 & 0 & 0 & -r^2\sin^2\theta \end{pmatrix}, \tag{12}$$

we describe the geodesic behavior of Schwarzschild-like wormholes by reconstructing Lagrangian, $\mathcal{L} = \frac{1}{2} g_{\alpha\beta} \frac{dx^\alpha}{d\tau}\frac{dx^\beta}{d\tau}$. From the metric in Equation (2), we have

$$\mathcal{L} = \frac{1}{2}\left\{ \dot{t}^2 - \frac{1}{(1-\beta)\left(1-\frac{r_0}{r}\right)}\dot{r}^2 - r^2\dot{\theta}^2 - r^2\sin^2\theta\dot{\phi}^2 \right\}. \tag{13}$$

By considering the test particle path confined to the plane $\theta = \pi/2$, we formulate the conserved conjugate momenta for t and ϕ component $\Pi_t = \frac{d\mathcal{L}}{d\dot{t}} = \dot{t} = E$ and $\Pi_\phi = -\frac{d\mathcal{L}}{d\dot{\phi}} = r^2\dot{\phi} = L$. The path of particle satisfy in the following

$$E^2 = \frac{1}{(1-\beta)\left(1-\frac{r_0}{r}\right)}\dot{r}^2 + \frac{L^2}{r^2} \tag{14}$$

for foton (null geodesics) and L is the angular momentum per unit mass, and

$$E^2 = 1 + \frac{1}{(1-\beta)\left(1-\frac{r_0}{r}\right)}\dot{r}^2 + \frac{L^2}{r^2} \tag{15}$$

for particle (timelike geodesics).

Now, we more explore the radial timelike geodesics for $L = 0$ in Eq. (15)

$$E^2 = 1 + \frac{1}{(1-\beta)\left(1-\frac{r_0}{r}\right)}\dot{r}^2, \tag{16}$$

we consider introducing the initial conditions where r_i and v_i are the initial position and velocity, respectively, from t_i. We shall suppose that the test particle from $t_i = 0$ at r_i starts to move with initial velocity v_i. These initial conditions imply

$$E^2 = 1 + \frac{1}{(1-\beta)\left(1-\frac{r_0}{r_i}\right)} v_i^2. \tag{17}$$

From Eq. (16) and (17), we have

$$v(r) = \pm\sqrt{\frac{\left(1-\frac{r_0}{r}\right)}{\left(1-\frac{r_0}{r_i}\right)}} v_i, \tag{18}$$

where the negative sign is valid for particles moving from r_i toward the wormhole throat and the positive sign is valid for particles moving from the wormhole throat to infinity. Eq. (18)follows that $r_i \geq r_0$ and the radial velocity is zero at $r = r_0$ (the throat). The particle acceleration is given by

$$a(r) = \frac{(1-\beta)(E^2-1)r_0}{2r^2}, \tag{19}$$

which is everywhere positive. Particle moves from their initial position r_i with initial velocity v_i toward the throat with decreasing velocity and arrive at r_0 (the throat) with zero velocity. Next, the particle moves from the throat r_0 with zero velocity toward infinity $r = \pm\infty$ with a maximum velocity, $v_{max} = \pm\frac{v_i}{\sqrt{\left(1-\frac{r_0}{r_i}\right)}}$. Figure 2 shows the particle velocity in a geodesic of a Schwarzschild-like wormhole.

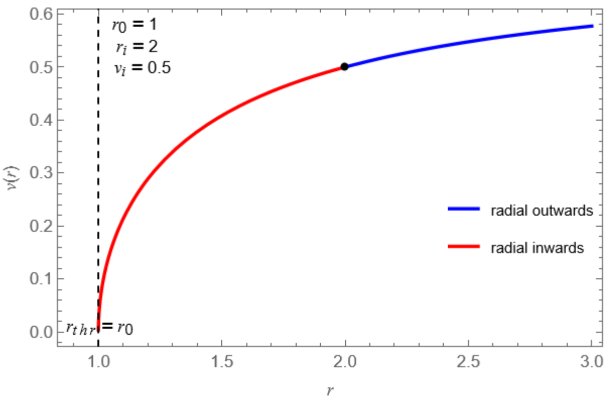

Figure 2. Velocity of particle $v(r)$ in Schwarzschild-like wormhole for $L = 0$.

We also explore the non-radial timelike geodesics where $L \neq 0$. The initial condition to be considered are position (r_i, ϕ_i), initial radial velocity v_i and initial angular velocity $\dot{\phi}_i$. The test particle starts from r_i with initial radial velocity v_i and initial angular velocity $\dot{\phi}_i$. The initial condition can be applied to Eq. (15) yields

$$E^2 = 1 + \frac{1}{(1-\beta)\left(1-\frac{r_0}{r_i}\right)} v_i^2 + \frac{L^2}{r_i^2}, \tag{20}$$

where $L = r^2\dot{\phi}$. The initial condition imply that a particle starts from r_i with an initial angular velocity $\dot{\phi}_i$ where $L = r_i^2\dot{\phi}_i$. From Eqs. (15) and (20), we obtain the radial velocity as follows:

$$v(r) = \pm\sqrt{(1-\beta)\left(1-\frac{r_0}{r}\right)\left[L^2\left(\frac{1}{r_i^2}-\frac{1}{r^2}\right)+\frac{1}{(1-\beta)\left(1-\frac{r_0}{r_i}\right)}v_i^2\right]}. \tag{21}$$

Eq. (21) is zero at $r_{01} = r_0$ (throat) and at

$$r_{02} = \left(\frac{1}{r_i^2} - \frac{1}{L^2(1-\beta)\left(1-\frac{r_0}{r_i}\right)}v_i^2\right)^{-\frac{1}{2}}. \tag{22}$$

For $L = 0$ in Eq. (21), the radial velocity reduces to the Eq. (18). The acceleration from Eq. 21 is given by

$$a(r) = (1-\beta)\left(1-\frac{r_0}{r}\right)\frac{L^2}{r^3}, \tag{23}$$

where $a(r) \geq 0$ is positive everywhere. For $r_{02} > r_{01}$ and $r_i > r_{01}$, a particle starts from $r_i = r_{02}$ with $v_i = 0$ to the point at $r_{01} < r < r_{02}$ and produces an imaginary velocity. The imaginary velocity has no physical meaning and it cannot be reached by the particle. Therefore, the point at r_{02} is a turning point where the particle escape to the infinity and the particle will never reach the wormhole throat at $r_{01} = r_0$ (not-traversable), see Figure 3.

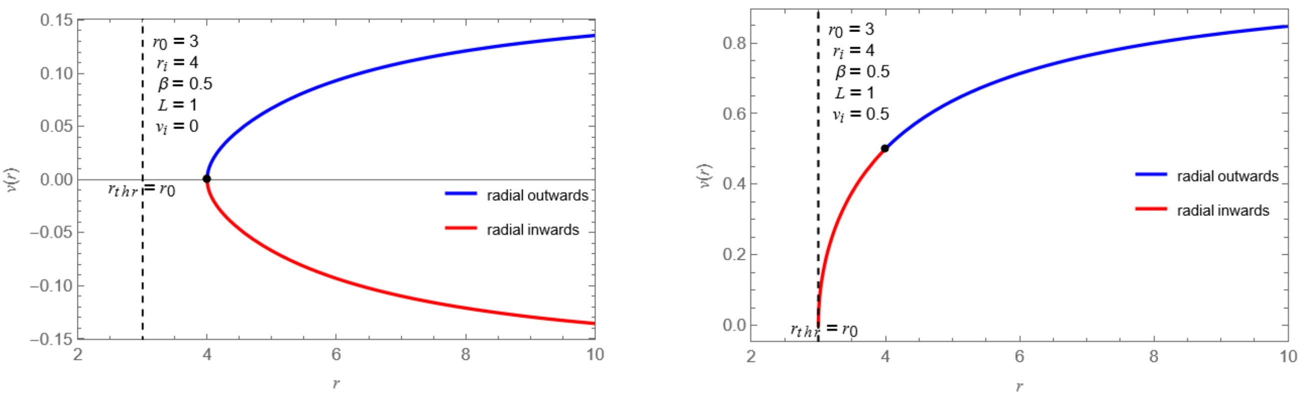

(a) (b)

Figure 3. Velocity of particle $v(r)$ with angular momentum L in Schwarzschild-like wormhole (a) for $v_i = 0$ and (b) for $v_i \neq 0$.

3. Isotropic Schwarzschild-like Wormhole

In this part, we will transform Eq. (2) into isotropic coordinates (t, ρ, θ, ϕ) by definition as follows:

$$ds^2 = dt^2 - F^2(\rho)[d\rho^2 + \rho^2 d\theta^2 + \rho^2 \sin^2\theta d\phi^2] \tag{24}$$

where $F(\rho)$ is a conformal factor to be determined later. By comparing the spatial line element, we have

$$r = \rho F(\rho) \quad \text{and} \quad \frac{dr}{d\rho} = F(\rho)\sqrt{(1-\beta)\left(1-\frac{r_0}{r}\right)}. \tag{25}$$

The relation of Eq. (25) is written as

$$\frac{dr}{r\sqrt{1-r_0/r}} = \sqrt{1-\beta}\frac{d\rho}{\rho}, \tag{26}$$

and suppose that $y^2 = 1 - \frac{r_0}{r}$ or $dr = \frac{2r_0 y}{(1-y^2)^2}dy$, we obtain

$$\int \frac{2dy}{1-y^2} = \int \sqrt{1-\beta}\frac{d\rho}{\rho}. \tag{27}$$

By solving the integral equation using some mathematical technique, we have

$$\ln\left|\frac{1+y}{1-y}\right| = \sqrt{1-\beta}\ln\rho + C, \tag{28}$$

and by taking $C = \ln D$, we solve Eq. (28) as follows:

$$y = \frac{D\rho^A - 1}{D\rho^A + 1}, \tag{29}$$

where $A = \sqrt{1-\beta}$. We return to the initial variable r by substituting equation (29) into $r = r_0/(1-y^2)$ reads:

$$r(\rho) = \frac{r_0}{4}(D^{1/2}\rho^{A/2} + D^{-1/2}\rho^{-A/2})^2. \tag{30}$$

The constant D is obtained by satisfying the Schwarzschild black hole condition: if $\beta = 0$, then $r_0 = 2m$. We obtain $D = \frac{4}{r_0}$ and the transformation of the Schwarzschild-like wormhole to the isotropic coordinates satisfies

$$r(\rho) = \rho^{\sqrt{1-\beta}}\left(1 + \frac{r_0}{4\rho^{\sqrt{1-\beta}}}\right)^2, \tag{31}$$

and the conformal factor is given by

$$F(\rho) = \rho^{\sqrt{1-\beta}-1}\left(1 + \frac{r_0}{4\rho^{\sqrt{1-\beta}}}\right)^2, \tag{32}$$

so the Schwarzschild-like wormhole in isotropic coordinate in Eq. (24) is written as

$$ds^2 = dt^2 - \rho^{2\left(\sqrt{1-\beta}-1\right)}\left(1 + \frac{r_0}{4\rho^{\sqrt{1-\beta}}}\right)^4\left(d\rho^2 + \rho^2 d\theta^2 + \rho^2\sin^2\theta d\phi^2\right). \tag{33}$$

The throat of metric in Eq. (33) is defined by the minimum of areal radius $R = \sqrt{|g_{\theta\theta}|}$. By setting $dr/d\rho = 0$, the throat is found at $\rho_{thr} = \left(\frac{r_0}{4}\right)^{1/\sqrt{1-\beta}}$ where the radius throat is $r_{thr} = r_0$.

We also analyze the singularity of metric (33) by calculating Kretschmann scalar $K = R_{\mu\nu\alpha\beta}R^{\mu\nu\alpha\beta}$ at $\rho = 0$, $\rho \to \infty$, and $\rho = \rho_{thr}$. The Kretschmann scalar curvatures K of the metrik Equation (33) are given by

$$K = \frac{(A'(\rho))^2}{A(\rho)^2} + \frac{4(1-A(\rho))^2}{A(\rho)^2} + \left(-\frac{A"(\rho)}{2A(\rho)} + \frac{(A'(\rho))^2}{4A(\rho)^2}\right)^2 + \frac{2}{A(\rho)^2\rho^4}\Bigg(-\frac{\rho A'(\rho)}{2} - \frac{\rho^2 A"(\rho)}{2} + \frac{\rho^2(A'(\rho))^2}{4A(\rho)}\Bigg)^2, \tag{34}$$

where A is the constant and the derivative of A is calculated as follows:

$$A(\rho) = \rho^{2(a-1)}\left(1+\frac{b_0}{4\rho^a}\right)^4 \tag{35}$$

$$A'(\rho) = 2\rho^{2(a-1)-1}\left(1+\frac{b_0}{4\rho^a}\right)^3\left(a-1-\frac{b_0}{4\rho^a}\right) \tag{36}$$

$$A''(\rho) = 2(2(a-1)-1)\rho^{2(a-1)-2}\left(1+\frac{b_0}{4\rho^a}\right)^3\left(a-1-\frac{b_0}{4\rho^a}\right) - 6a\frac{b_0}{4}\rho^{2(a-1)-a-2}\left(1+\frac{b_0}{4\rho^a}\right)^2 \times\left(a-1-\frac{b_0}{4\rho^a}\right) + 2a\frac{b_0}{4}\rho^{2(a-1)-a-2}\left(1+\frac{b_0}{4\rho^a}\right)^3. \tag{37}$$

From the Kretschmann scalar, we obtain that the point at $\rho = 0$ is a curvature singularity but the domain of the coordinate allows $\rho_{thr} \leq \rho \leq \infty$ and $\rho_{thr} > 0$. The objects never reach the throat because the minimal radius is exceeded at ρ_{thr}. In conclusion, there is no singularity for $\rho_{thr} \leq \rho \leq \infty$ because the Kretschmann scalar is finite. The true singularity happens in the limit $\beta \to 1$ where the metric is divergent for arbitrary value of ρ.

Assuming a matter source threading the wormhole is described by anisotropic fluid with energy-momentum tensor $T^{\nu}_{\mu} = \mathrm{diag}(\rho, -p_r, -p_l, -p_l)$, we obtain the Einstein field equations in the following

$$\kappa\rho = -\,\frac{1+2A(\rho)}{4A(\rho)^2}\,A''(\rho) \;-\; \frac{A'(\rho)}{2A(\rho)\rho} \;+\; \frac{1+2A(\rho)}{8A(\rho)^3}\,(A'(\rho))^2, \tag{38}$$

$$\kappa p_r = -\,\frac{2A(\rho)-1}{4A(\rho)^2}\,A''(\rho) \;-\; \frac{A'(\rho)}{2A(\rho)\rho} \;-\; \frac{1-2A(\rho)}{8A(\rho)^3}\,(A'(\rho))^2, \tag{39}$$

$$\kappa p_\ell = -\,\frac{1}{4A(\rho)^2}\,A''(\rho) \;+\; \frac{1}{8A(\rho)^3}\,(A'(\rho))^2. \tag{40}$$

From the above calculation, we obtain that $\kappa(\rho + p_r) < 0$ and $\kappa(\rho + p_\ell) < 0$. The conditions violate the Energy Condition: Null Energy Condition (NEC), Weak Energy Condition (WEC), and Strong Energy Condition (SEC). Furthermore, the Dominant Energy Condition (DEC) is also violated because we find that $|p_r|, |p_\ell| > \rho$ because it does not satisfy DEC condition $|p_i| \leq \rho$ where i is the radial and lateral component. So, all standard energy conditions are violated in isotropic coordinates. This results are similar with Schwarzschild-like wormholes and consistent with the properties of traversable wormholes. This violation allows the presence of exotic matter that produces energy with a negative value.

3.1. The Embedding of Schwarzschild-like Wormholes In Isotropic Coordinate

The Schwarzschild-like wormhole metric in isotropic coordinate as Eq. (33) is embedded into cylindrical spacetime $(t, \rho_s, \theta, \phi)$. For $t =$ const and $\theta = \pi/2$, the metric is given by

$$\rho_s^2 + dz^2 + \rho_s^2 d\phi^2 = \rho^{2\left(\sqrt{1-\beta}-1\right)}\left(1+\frac{r_0}{4\rho^{\sqrt{1-\beta}}}\right)^4\left(d\rho^2 + \rho^2 d\phi^2\right). \tag{41}$$

Journal of Physics: Conference Series **3238** (2026) 012048 doi:10.1088/1742-6596/3238/1/012048

By comparing the two sides of Eq. (41), we obtain the relation

$$\rho_s = \rho^{2\sqrt{1-\beta}} \left(1 + \frac{r_0}{4\rho^{\sqrt{1-\beta}}}\right)^4, \tag{42}$$

$$dz^2 + d\rho_s^2 = \rho^{2\left(\sqrt{1-\beta}-1\right)} \left(1 + \frac{r_0}{4\rho^{\sqrt{1-\beta}}}\right)^4 d\rho^2. \tag{43}$$

From Equation (42) and (43), we have the embedding function as follows:

$$\frac{dz}{d\rho} = \sqrt{A^2(\rho) - \frac{dR^2(\rho)}{d\rho^2}}, \tag{44}$$

where $A(\rho)$ and $R(\rho)$ are given by

$$A(\rho) = \rho^{\left(\sqrt{1-\beta}-1\right)} \left(1 + \frac{r_0}{4\rho^{\sqrt{1-\beta}}}\right)^2, \tag{45}$$

$$R(\rho) = \rho^{\sqrt{1-\beta}} \left(1 + \frac{r_0}{4\rho^{\sqrt{1-\beta}}}\right)^2, \tag{46}$$

and the embedding function reads:

$$z = \int \sqrt{\rho^{2\left(\sqrt{1-\beta}-1\right)} \left(1 + \frac{r_0}{4\rho^{\sqrt{1-\beta}}}\right)^4 - \frac{dR^2(\rho)}{d\rho^2}} d\rho. \tag{47}$$

We show a plot of the embedding diagram of Schwarzschild-like wormhole in isotropic coordinate from Eq. (47) as Figure 4.

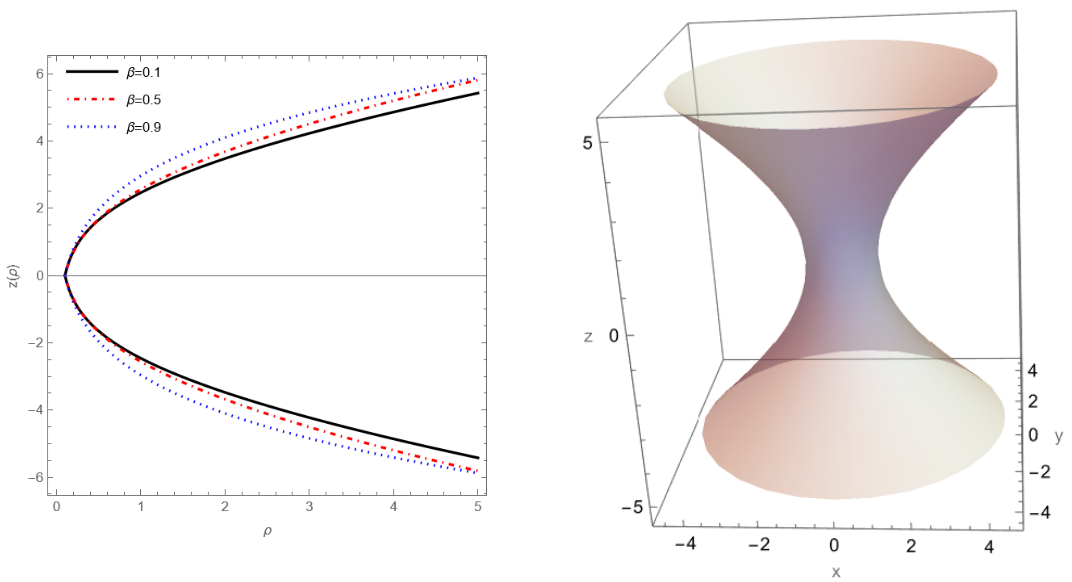

Figure 4. Embedding diagram of a isotropic Schwarzschild-like wormhole (a) 2D and (b) 3D

Journal of Physics: Conference Series **3238** (2026) 012048 doi:10.1088/1742-6596/3238/1/012048

3.2. The Geodesic of Isotropic Schwarzschild-like Wormhole

The metric component of the Schwarzschild-like wormhole in isotropic coordinates is given by

$$g_{\alpha\beta} = \begin{pmatrix} 1 & 0 & 0 & 0 \\ 0 & -F^2(\rho) & 0 & 0 \\ 0 & 0 & -\rho^2 F^2(\rho) & 0 \\ 0 & 0 & 0 & -\rho^2 \sin^2\theta F^2(\rho) \end{pmatrix}, \tag{48}$$

where

$$F^2(\rho) = \rho^{2(\sqrt{1-\beta}-1)} \left(1 + \frac{r_0}{4\rho^{\sqrt{1-\beta}}}\right)^4. \tag{49}$$

We describe the geodesic behavior of Schwarzschild-like wormholes in isotropic coordinates by constructing a Lagrangian $\mathcal{L} = \frac{1}{2} g_{\alpha\beta} \frac{dx^\alpha}{d\tau}\frac{dx^\beta}{d\tau}$. From the metric in Eq. (48), we obtain

$$\mathcal{L} = \frac{1}{2}\{\dot{t}^2 - F^2(\rho)\dot{\rho}^2 - \rho^2 F^2(\rho)\dot{\theta}^2 - \rho^2\sin^2\theta F^2(\rho)\dot{\phi}^2\}. \tag{50}$$

The conserved conjugate momenta for t and ϕ component are written as $\Pi_t = \frac{d\mathcal{L}}{d\dot{t}} = \dot{t} = E$ and $\Pi_\phi = -\frac{d\mathcal{L}}{d\dot{\phi}} = \rho^2 F^2(\rho)\dot{\phi} = L$, respectively. We shall consider the test particle paths confined to the plane $\theta = \pi/2$ and the path of particle in isotropic coordinate is formulated as follows:

$$E^2 = F^2(\rho)\dot{\rho}^2 + \frac{L^2}{\rho^2 F^2(\rho)}, \tag{51}$$

for foton (lightlike) and for particle (timelike) as follows:

$$E^2 = 1 + F^2(\rho)\dot{\rho}^2 + \frac{L^2}{\rho^2 F^2(\rho)}, \tag{52}$$

where L is the angular momentum per unit mass. We more explore radial timelike geodesics for $L = 0$ and we have

$$\dot{\rho}^2 = \frac{E^2 - 1}{F^2(\rho)}, \tag{53}$$

where $F(\rho)$ is presented by Eq. (49). We also introduce the initial position of particle at ρ_i and $t_i = 0$, where the particle starts with the initial velocity v_i. The initial conditions imply that

$$\dot{\rho}_i^2 = \frac{E^2 - 1}{F^2(\rho_i)}. \tag{54}$$

From Eqs. (53) and (54), we have the velocity of partcle as follows:

$$v(\rho) = \pm \left(\frac{\rho_i}{\rho}\right)^{(\sqrt{1-\beta}-1)} \left(\frac{1 + \frac{r_0}{4\rho_i^{\sqrt{1-\beta}}}}{1 + \frac{r_0}{4\rho^{\sqrt{1-\beta}}}}\right)^2 v_i, \tag{55}$$

where the negative sign is valid for particles moving from ρ_i toward the throat and the positive sign for particles move from the throat to infinity. We also calculate the acceleration for particle by taking the second derivative of Eq. (55)

$$a(\rho) = \frac{(E^2-1)\,\rho^{-2(\sqrt{1-\beta}-1)-1}}{2} \left(1 + \frac{r_0}{4\rho^{\sqrt{1-\beta}}}\right)^{-5} \left[-2\left(\sqrt{1-\beta}-1\right) + \frac{(\sqrt{1-\beta}+1)\,r_0}{2\rho^{\sqrt{1-\beta}}}\right], \tag{56}$$

where the value is everywhere positive for $0 < \beta < 1$, $r_0 > 0$ and $E > 0$. The particle moves from ρ_i with initial velocity v_i toward the throat $\rho_{thr} = \left(\frac{r_0}{4}\right)^{1/\sqrt{1-\beta}}$ and arrives at the throat with velocity

$$v(\rho_{\rm thr}) \;=\; \pm\left(\frac{\rho_i}{\left(\frac{r_0}{4}\right)^{1/\sqrt{1-\beta}}}\right)^{\sqrt{1-\beta}-1}\left(\frac{1+\dfrac{r_0}{4\rho_i^{\sqrt{1-\beta}}}}{2}\right)^2 v_i. \tag{57}$$

Next, the particles move from the throat toward infinity $\rho \to \pm\infty$ with a maximum velocity close to infinity. Figure 5 shows the particle velocity in a geodesic of a Schwarzschild-like wormhole in coordinate isotropic.

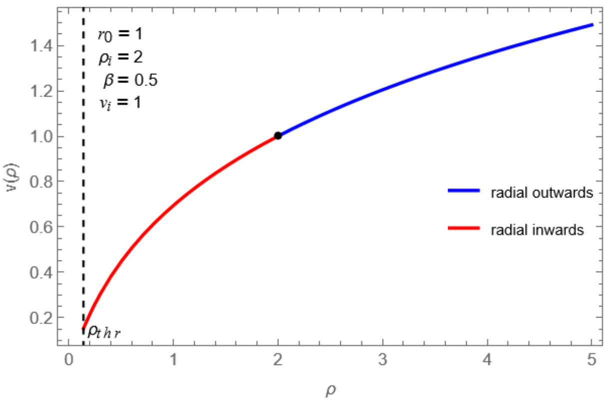

Figure 5. Velocity of particle $v(\rho)$ in isotropic Schwarzschild-like wormhole for $L = 0$.

Then, we explore for a non-radial timelike geodesic where $L \neq 0$. The initial position of particle at ρ_i and $t_i = 0$, where the particle starts with the initial radial velocity v_i and initial angular velocity $\dot{\phi}_i$. The initial condition is substituted to the Eq. (52) yield

$$E^2 = 1 + F^2(\rho_i)\dot{\rho_i}^2 + \frac{L^2}{\rho_i^2 F^2(\rho_i)}, \tag{58}$$

where $L = \rho^2 F^2(\rho)\dot{\phi}$ is the angular momentum per unit mass. From Eqs. (52) and (58), we obtain the velocity as follows:

$$v(\rho) = \pm\sqrt{\frac{F^2(\rho_i)}{F^2(\rho)}\,\dot{\rho_i}^2 \;+\; \frac{L^2}{F^2(\rho)}\left(\frac{1}{\rho_i^2 F^2(\rho_i)} - \frac{1}{\rho^2 F^2(\rho)}\right)}. \tag{59}$$

By substituting Eq. (49) to the Eq. (59), we obtain the complete form of velocity in the following

$$v(\rho) = \pm\sqrt{\frac{\rho_i^{2(\sqrt{1-\beta}-1)}\left(1+\dfrac{r_0}{4\rho_i^{\sqrt{1-\beta}}}\right)^4 v_i^2 + L^2\left[\rho_i^{-2\sqrt{1-\beta}}\left(1+\dfrac{r_0}{4\rho_i^{\sqrt{1-\beta}}}\right)^{-4} - \rho^{-2\sqrt{1-\beta}}\left(1+\dfrac{r_0}{4\rho^{\sqrt{1-\beta}}}\right)^{-4}\right]}{\rho^{2(\sqrt{1-\beta}-1)}\left(1+\dfrac{r_0}{4\rho^{\sqrt{1-\beta}}}\right)^4}}. \tag{60}$$

For $L = 0$, the velocity in Eq. (60) reduces to the Eq. (55). The acceleration of particle is defined by taking the differential of velocity and the result is as follows:

$$
\begin{aligned}
a(\rho) = {} & \frac{1}{2\left[\rho^{2(\sqrt{1-\beta}-1)}\left(1+\frac{r_0}{4\rho^{\sqrt{1-\beta}}}\right)^4\right]^2}\Bigg\{\Bigg[2\sqrt{1-\beta}\,L^2\,\rho^{-2\sqrt{1-\beta}-1}\left(1+\frac{r_0}{4\rho^{\sqrt{1-\beta}}}\right)^{-4} \\
& - r_0\sqrt{1-\beta}\,L^2\,\rho^{-3\sqrt{1-\beta}-1}\left(1+\frac{r_0}{4\rho^{\sqrt{1-\beta}}}\right)^{-5}\Bigg]\rho^{2(\sqrt{1-\beta}-1)}\left(1+\frac{r_0}{4\rho^{\sqrt{1-\beta}}}\right)^4 \\
& - \left[\rho_i^{2(\sqrt{1-\beta}-1)}\left(1+\frac{r_0}{4\rho_i^{\sqrt{1-\beta}}}\right)^4 v_i^2 + L^2\left(\rho_i^{-2\sqrt{1-\beta}}\left(1+\frac{r_0}{4\rho_i^{\sqrt{1-\beta}}}\right)^{-4} - \rho^{-2\sqrt{1-\beta}}\left(1+\frac{r_0}{4\rho^{\sqrt{1-\beta}}}\right)^{-4}\right)\right] \\
& \times\left[2(\sqrt{1-\beta}-1)\rho^{2\sqrt{1-\beta}-3}\left(1+\frac{r_0}{4\rho^{\sqrt{1-\beta}}}\right)^4 - r_0\sqrt{1-\beta}\,\rho^{\sqrt{1-\beta}-3}\left(1+\frac{r_0}{4\rho^{\sqrt{1-\beta}}}\right)^3\right]\Bigg\},
\end{aligned}
\tag{61}
$$

where $a(r) > 0$ is positive everywhere. If $v_i = 0$, the velocity of particle becomes zero at $\rho = \rho_i$ and the velocity at $\rho_{rth} < \rho < \rho_i$ has an imaginary value which is no physical meaning. The particle never reach the throat and move toward infinite (radially outward).

The turning point occurs at ρ_i and the angular momentum affects to the circular motion of particle to the radial outward. If $v_i \neq 0$, the particle has sufficient kinetic energy to reach the throat and pass through the wormhole throat to another spacetime, see Figure 6. The initial velocity is a determining factor in whether a particle can reach the throat. In addition to angular momentum, the particle needs sufficient energy to reach the throat through a traversable wormhole. Angular momentum indicates that the particle's motion toward the throat is accompanied by tangential motion resulting in a circular trajectory. In contrast, if the angular momentum is zero, the particle moves directly toward the throat. Only particles with sufficiently small angular momentum can penetrate the throat.

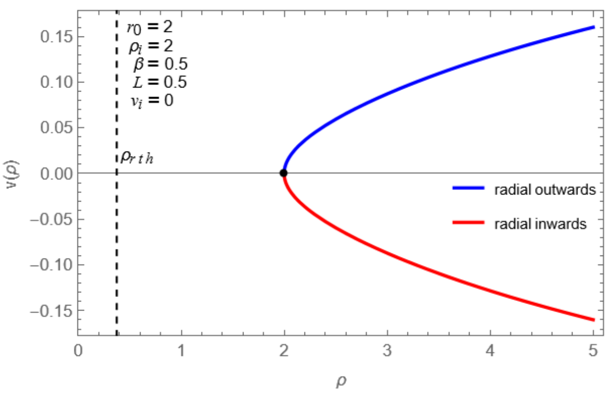

(a)

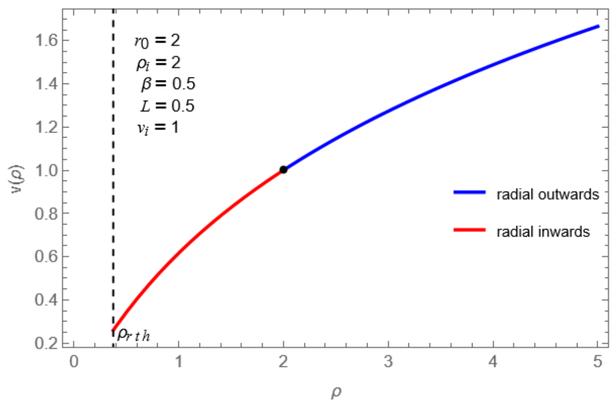

(b)

Figure 6. Velocity of particle $v(r)$ with angular momentum L in isotropic Schwarzschild-like wormhole (a) for $v_i = 0$ and (b) for $v_i \neq 0$.

4. Conclusions

We have studied the traversability of a Schwarzschild-like wormhole in isotropic coordinates. The isotropic form of the metric provides a comprehensive description of the two asymptotic regions through a throat of the wormhole, and the stability of the throat prevents singularities from appearing in spacetime (nonsingular), so the wormhole remains traversable. Although the isotropic representation confirms the traversable nature of the wormhole, traversability is strongly constrained by angular momentum and initial velocity, since a centrifugal barrier can prevent crossing toward the throat. Our results demonstrate that the initial velocity plays a crucial role in determining whether a particle is trapped or allowed to pass through the wormhole throat. When $v_i = 0$, the particle has no initial kinetic energy and its dynamics are governed solely by the wormhole curvature, which tends to confine the trajectory near the starting point. In contrast, for $v \neq 0$, the particle possesses kinetic energy that allows it to overcome potential barriers, approach the throat, and, in some cases, traverse to the other side. The practical potential analysis reveals that nonzero angular momentum introduces a centrifugal barrier, which can prevent particles from reaching the throat, whereas purely radial ($L \neq 0$) trajectories allow traversal.

Future work may focus on extending this analysis to charged or rotating wormholes, examining the stability of such geometries under perturbations, and exploring observational signatures in realistic astrophysical environments. Such studies could provide crucial steps toward assessing the physical viability and detectability of Schwarzschild-like wormholes.

References

[1] Cataldo M, Liempi L and Rodríguez P 2017 *Eur. Phys. J. C* **77** 11
[2] Flamm L 1916 *Physikalische Zeitschrift* **17** 448-454
[3] Weyl H 1928 *Beiträge zur Einsteinschen gravitationstheorie* (Leibniz Verlag)
[4] Weyl H 1949 *Philosophy of Mathematics and Natural Science* (Princeton University Press)
[5] Einstein A and Rosen N 1935 *Phys. Rev.* **48** 73
[6] Frolov V P and Novikov I D 1990 *Phys. Rev. D* **42** 1057
[7] Misner C W and Wheeler J A 1957 *Ann. of phys.* **2** 525-60
[8] Hawking S and Ellis H G 1973 *The Large Scale Structure of Space-Time* (Cambridge University Press)
[9] Misner C W, Thorne K and Wheeler J 1978 *Gravitation* (San Francisco: Freeman)
[10] Wald R 2010 *General relativity* (University of Chicago press)
[11] Ellis H G 1973 *J. Math. Phys.* **14** 104-118
[12] Ellis H G 2004 The warp drive and antigravity *preprint* gr-qc/0411096
[13] Morris M and Thorne K *American J.* **56** 395-412
[14] Teo E 1998 *Phys. Rev. D* **58** 024014
[15] Santos A C L, Muniz C R and Oliveira L T 2021 *Inter. J. Mod. Phys. D* **30** 2150032